

Short Note

# 3-(5-Phenyl-2H-tetrazol-2-yl)pyridine

Ivan S. Ershov <sup>1</sup>, Kirill A. Esikov <sup>1</sup>, Olga M. Nesterova <sup>1</sup>, Mariya A. Skryl'nikova <sup>1,2</sup>, Andrey V. Khranchikhin <sup>2</sup> ,  
Nadezda T. Shmaneva <sup>1</sup>, Ivan S. Chernov <sup>1</sup>, Ekaterina N. Chernova <sup>3</sup> , Aleksandra M. Puzyk <sup>4</sup> ,  
Eugene V. Sivtsov <sup>5</sup> , Yuliya N. Pavlyukova <sup>1</sup>, Rostislav E. Trifonov <sup>1</sup> and Vladimir A. Ostrovskii <sup>1,3,\*</sup> 

- <sup>1</sup> Department of Chemistry and Technology of Nitrogen-Containing Organic Compounds, Saint Petersburg State Institute of Technology (Technical University), 24-26/49 Moskovsky Ave., 190013 St. Petersburg, Russia  
<sup>2</sup> Department of Organic Chemistry, Saint Petersburg State Institute of Technology (Technical University), 24-26/49 Moskovsky Ave., 190013 St. Petersburg, Russia  
<sup>3</sup> Saint Petersburg Federal Research Center of the Russian Academy of Sciences (SPC RAS), 39, 14th Line, 199178 St. Petersburg, Russia  
<sup>4</sup> Research Park, Saint Petersburg State University, 26 Universitetskii Prospekt, Petergof, 198504 St. Petersburg, Russia  
<sup>5</sup> Department of Physical Chemistry, Saint Petersburg State Institute of Technology (Technical University), 24-26/49 Moskovsky Ave., 190013 St. Petersburg, Russia  
\* Correspondence: va\_ostrovskii@mail.ru; Tel.: +7-921-953-0789

**Abstract:** 3-(5-Phenyl-2H-tetrazol-2-yl)pyridine was synthesized by treating 5-phenyl-1H-tetrazole with pyridin-3-ylboronic acid under Chan–Evans–Lam coupling conditions. The structure and identity were confirmed by <sup>1</sup>H, <sup>13</sup>C-NMR spectroscopy, IR spectroscopy, UV–Vis spectroscopy, high-resolution mass spectrometry, and TLC. The molecular structure was studied experimentally by sequential X-ray diffraction analysis and theoretically by DFT B3LYP quantum chemistry calculation.

**Keywords:** 3-(5-phenyl-2H-tetrazol-2-yl)pyridine; synthesis; molecular structure; X-ray diffraction analysis; quantum chemistry calculation; NMR spectroscopy; IR spectroscopy; UV–Vis spectroscopy; mass spectrometry; quantum chemical calculation



**Citation:** Ershov, I.S.; Esikov, K.A.; Nesterova, O.M.; Skryl'nikova, M.A.; Khranchikhin, A.V.; Shmaneva, N.T.; Chernov, I.S.; Chernova, E.N.; Puzyk, A.M.; Sivtsov, E.V.; et al. 3-(5-Phenyl-2H-tetrazol-2-yl)pyridine. *Molbank* **2023**, *2023*, M1598. <https://doi.org/10.3390/M1598>

Academic Editor: Rodrigo Abonia

Received: 9 February 2023

Revised: 22 February 2023

Accepted: 25 February 2023

Published: 28 February 2023



**Copyright:** © 2023 by the authors. Licensee MDPI, Basel, Switzerland. This article is an open access article distributed under the terms and conditions of the Creative Commons Attribution (CC BY) license (<https://creativecommons.org/licenses/by/4.0/>).

## 1. Introduction

Tetrazoles are the most nitrogen-rich azoles and used as active ingredients in modern medicines, and as components of energy-saturated systems and functional materials [1]. Tetrazole derivatives are the active ingredients of highly effective drugs circulating in the modern world pharmaceutical market. For example, these are antihypertensive drug (losartan), cephalosporin antibiotic (latamoxef), histamine receptor blocker (2 h, 3 h) (pemirolast), and analgesic alfentanil (Figure 1) [2].

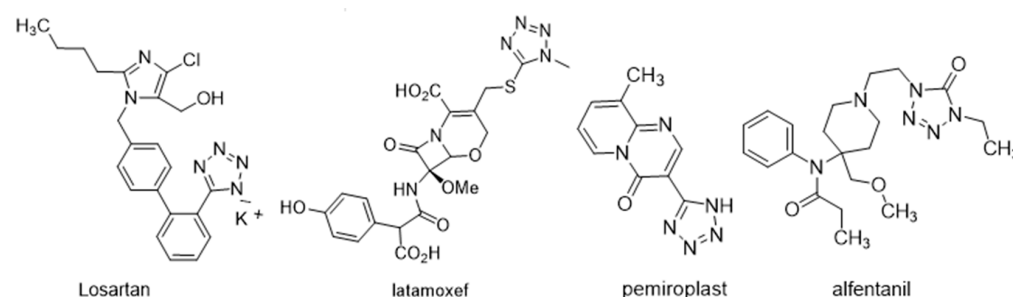


**Figure 1.** Examples of active ingredients of tetrazolyl-containing drugs.

The manifestations of such different biological activity are associated with the unique features of the high-nitrogen tetrazole ring. It is known that the tetrazole cycle is a bioisosteric analog of the cis-amide and carboxyl groups, which ensures the high metabolic

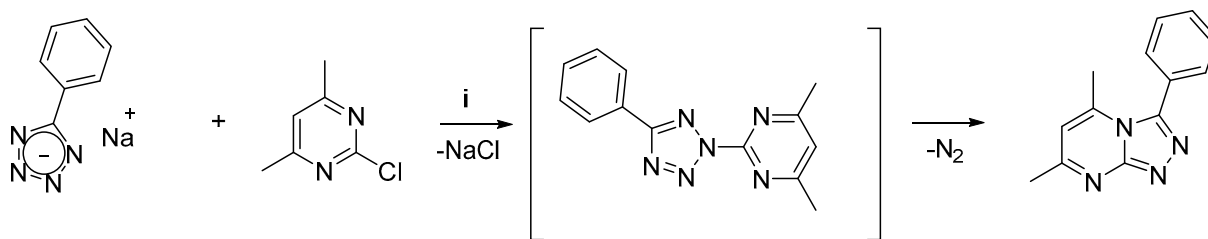
stability of tetrazole derivatives [3]. An important property of tetrazoles is the participation of “pyrrole-like” (NH group) and “pyridine-like” nitrogen atoms of the ring of types in the formation of multiple hydrogen bonds with the molecular structures of active sites of biological targets [2,4].

As follows from the above formulas, the active ingredients of most tetrazole-containing drugs are often “hybrid” heterocyclic systems containing, in addition to the tetrazole, at least one more heterocyclic fragment connected to the tetrazole ring by a bridge group (linker), sometimes having a rather complex structure. There is much less information about “hybrid” heterocyclic systems, in which the tetrazole ring and the “other” heterocyclic fragment are connected by a simple covalent bond. At the same time, it is precisely for such “hybrid” heterocyclic systems that multitarget biological activity should be expected.

Here, we preliminarily analyzed the data of computer prediction of the biological activity of 3-(5-phenyl-2*H*-tetrazol-2-yl)pyridine **1**, obtained using the PASS complex (Prediction of Activity Spectra for Substances), where  $P_a$  is the probability of presence, and  $P_i$  is the absence of a type of biological activity [5]. As follows from the data, 3-(5-phenyl-2*H*-tetrazol-2-yl)pyridine **1** can exhibit multitarget biological activity with a probability close to 80% as analgesic and neoioid ( $P_a = 0.795$ ;  $P_i = 0.005$ ), glycosylphosphatidylinositol inhibitor of phospholipase D ( $P_a = 0.788$ ;  $P_i = 0.015$ ), antagonist of nicotine receptors alpha-6-beta-3-beta-4-alpha-5 ( $P_a = 0.747$ ;  $P_i = 0.022$ ), and nicotine receptor antagonist alpha-2-beta-2 ( $P_a = 0.742$ ;  $P_i = 0.019$ ). The data obtained allow us to speak about the feasibility of synthesizing compound **1** and study its structural parameters, followed by studying the biological activity.

In order to conduct experimental testing of the biological activity of compound **1**, it is necessary to develop an efficient and safe method for its synthesis based on direct hetarylation of available 5-phenyl-1*H*-tetrazole.

Generally, direct arylation and hetarylation of 5*R*-tetrazoles are significantly hindered due to the low mobility of the halogen in the arylation (hetarylation) reagent to nucleophilic substitution. Other adverse factors should also be taken into account. For example, the low selectivity of the process due to the regioisomeric nature of *N*-aryl derivatives of 5*R*-tetrazoles. Often, direct hetarylation of 5*R*-tetrazoles with hetaryl halides is complicated by side processes due to the thermal lability of the intermediates. For example, when trying to synthesize 4,6-dimethyl-2-(5-phenyl-2*H*-tetrazol-2-yl)pyrimidine by direct hetarylation of the sodium salt of 5-phenyl-1*H*-tetrazole with 2-chloro-4,6-dimethylpyrimidine, 5,7-dimethyl-3-phenyl-[1,2,4]triazolo[4,3-*a*]pyrimidine was obtained instead of unannulated tetrazolypyrimidine. A possible reason for the observed phenomenon is the thermolytic recycling of the intermediate 6-dimethyl-2-(5-phenyl-2*H*-tetrazol-2-yl)pyrimidine, accompanied by the elimination of the  $N_2$  molecule and the formation of annulated triazolypyrimidine (Scheme 1) [6].

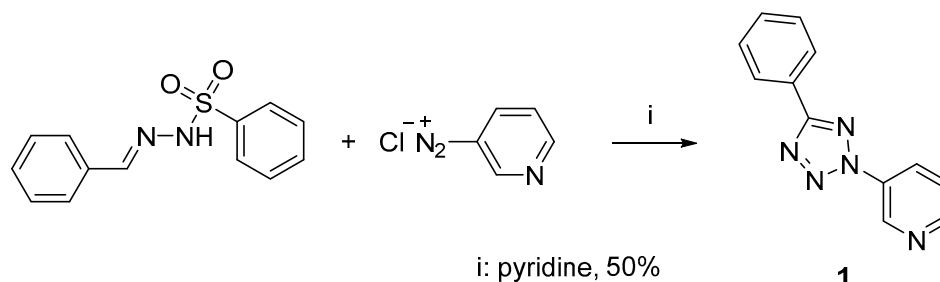


i, DMSO, 150°C, 8 h, 91%

**Scheme 1.** Synthesis of 5,7-dimethyl-3-phenyl-[1,2,4]triazolo[4,3-*a*]pyrimidine by hetarylation of the 5-phenyl-1*H*-tetrazole sodium salt with 2-chloro-4,6-dimethylpyrimidine.

Classical methods for the synthesis of 2,5-diaryltetrazoles are based on the reactions of arylidenearylsulfonylhydrazides with diazonium salts [7]. It is highly inexpedient to extend this method to the synthesis of 2-hetaryltetrazoles, since for this purpose it will be necessary to use reagents that are inaccessible and, in some cases, dangerous to handle.

An illustrative example is the synthesis of a representative of the 2-heteryl-5R-tetrazole series—3-(5-phenyl-2*H*-tetrazol-2-yl)pyridine **1**, published in [8]. The final stage of the multistage synthesis of compound **1** is shown below (Scheme 2).



**Scheme 2.** The final step in the synthesis of 3-(5-phenyl-2*H*-tetrazol-2-yl)pyridine **1** based on the reaction of the pyridine-3-diazonium salt on *N'*-benzylidenebenzenesulfonylhydrazide.

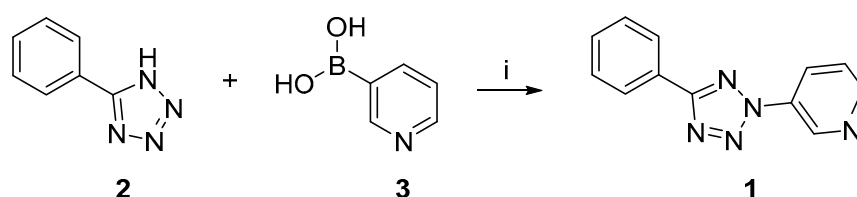
N2-Arylation of 5R-tetrazoles with diaryliodonium salts also cannot claim the status of a practically acceptable method due to the peculiarities of the synthesis and the complex handling of these arylizing agents [9]. We suggested that the most promising alternative to direct hetarylation of 5R-tetrazoles could be Chan–Evans–Lam cross-coupling, which is analogous to *O*- and *N*-arylation of nitrogenous bases (nucleophiles) with heterylboronic acids [10–12]. Arylation of various *N*-nucleophiles under the conditions of Chan–Evans–Lam cross-coupling has recently attracted increasing attention of researchers due to its high selectivity and relatively mild reaction conditions [13–17]. Successful examples of selective N2-arylation [18] and N2-vinylation of 5R-tetrazoles under Chan–Evans–Lam cross-coupling conditions turned out to be the most useful for this work [19]. The results obtained by Han et al. [20], which we chose as prototypes to achieve the goal of the work, had the greatest influence on our choice.

The aim of this work is the synthesis of 3-(5-phenyl-2*H*-tetrazol-2-yl)pyridine **1** using copper-catalyzed aerobic oxidative coupling of 5-phenyl-1*H*-tetrazole with pyridine-3-ylboronic acid.

## 2. Results and Discussion

### 2.1. Synthesis of 3-(5-Phenyl-2*H*-tetrazol-2-yl)pyridine **1**

We implemented Cu-catalyzed coupling of 5-phenyl-1*H*-tetrazole **2** with pyridine-3-ylboronic acid **3** under the conditions recommended in [20] and obtained 3-(5-phenyl-2*H*-tetrazol-2-yl)pyridine **1** in 87% yield (Scheme 3).



i: Cu<sub>2</sub>O (5 mol.%), O<sub>2</sub> (1 atm.), DMSO (dry), 100 °C, 4Å MS, 15h, 87%

**Scheme 3.** Synthesis of 3-(5-phenyl-2*H*-tetrazol-2-yl)pyridine **1** by hetarylation of 5-phenyl-1*H*-tetrazole **2** with pyridine-3-ylboronic acid **3** in DMSO.

We consider that this method for the synthesis of 3-(5-phenyl-2*H*-tetrazol-2-yl)pyridine **1** is characterized by the availability and safety of reagents, a smaller number of stages compared to the method described in [8]. We further described in detail a sample of previously inaccessible 3-(5-phenyl-2*H*-tetrazol-2-yl)pyridine **1**, using the instrumental and theoretical methods of investigation.

Samples of 3-(5-phenyl-2H-tetrazol-2-yl)pyridine **1** will be further transferred for experimental testing of biological activity in accordance with computer prediction data given above.

## 2.2. Differential Scanning Calorimetry (DSC)

After purification of a sample of compound **1** by column chromatography and additional crystallization (benzene/octan 1:1), we obtained melting points that differ markedly from each other. The melting point value obtained in the capillary is 125–126 °C, using the Kofler table—122–123 °C. The highest value of the melting point is 128–129 °C, indicated in the article [8]. To obtain objective information on the melting point of 3-(5-phenyl-2H-tetrazol-2-yl)pyridine **1**, we used differential scanning calorimetry data. The method makes it possible to record with high accuracy the thermal effects that occur during slow (1°/min) heating of a small sample of a substance (up to 2 mg), which makes it possible to accurately fix the onset of melting. The melting point was determined to be  $120.3 \pm 0.2$  °C (Figure 2). Such a difference in the obtained value of the melting temperature can be due to the minimization of the heating inertia of a small sample of the substance with effective control of the heating rate. The specific heat of fusion determined from the DSC thermograms is  $119 \pm 2$  J/g.

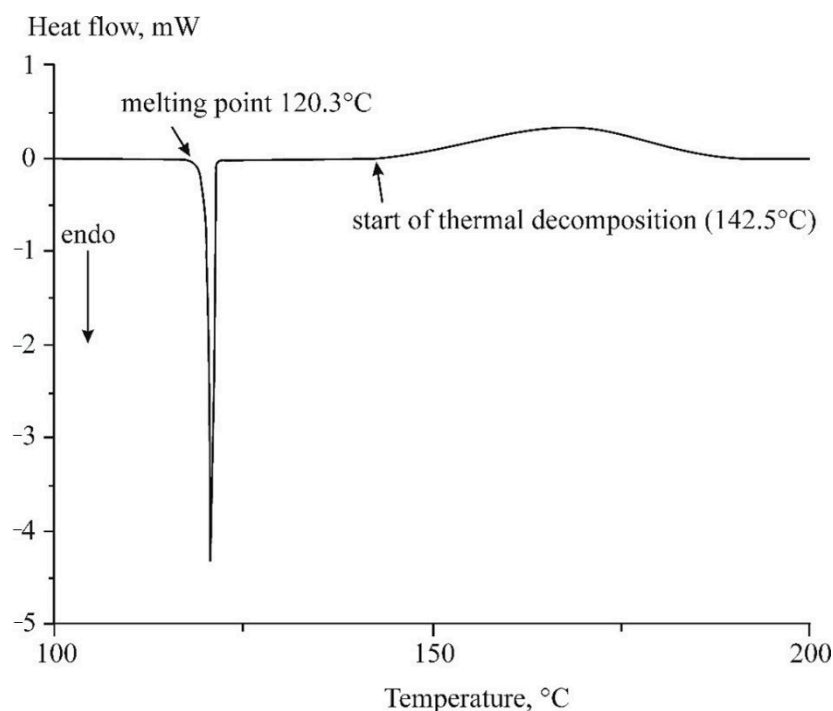


**Figure 2.** DSC thermogram of 3-(5-phenyl-2H-tetrazol-2-yl)pyridine **1**.

A peculiarity of the thermal decomposition of 2,5-disubstituted tetrazoles is the ease of elimination of N<sub>2</sub>, leading to the formation of nitrilimines in various structures [21–23]. This is the reason for the low thermal stability of 3-(5-phenyl-2H-tetrazol-2-yl)pyridine **1**. After passing into the melt, it undergoes thermal degradation at 142.5 °C, which is recorded in the DSC thermograms as an exo peak.

## 2.3. X-ray Diffraction Analysis and Quantum Chemistry Calculation

The spatial structure of 3-(5-phenyl-2H-tetrazol-2-yl)pyridine **1** was recorded in solid state. The structure is shown in Figure 3.

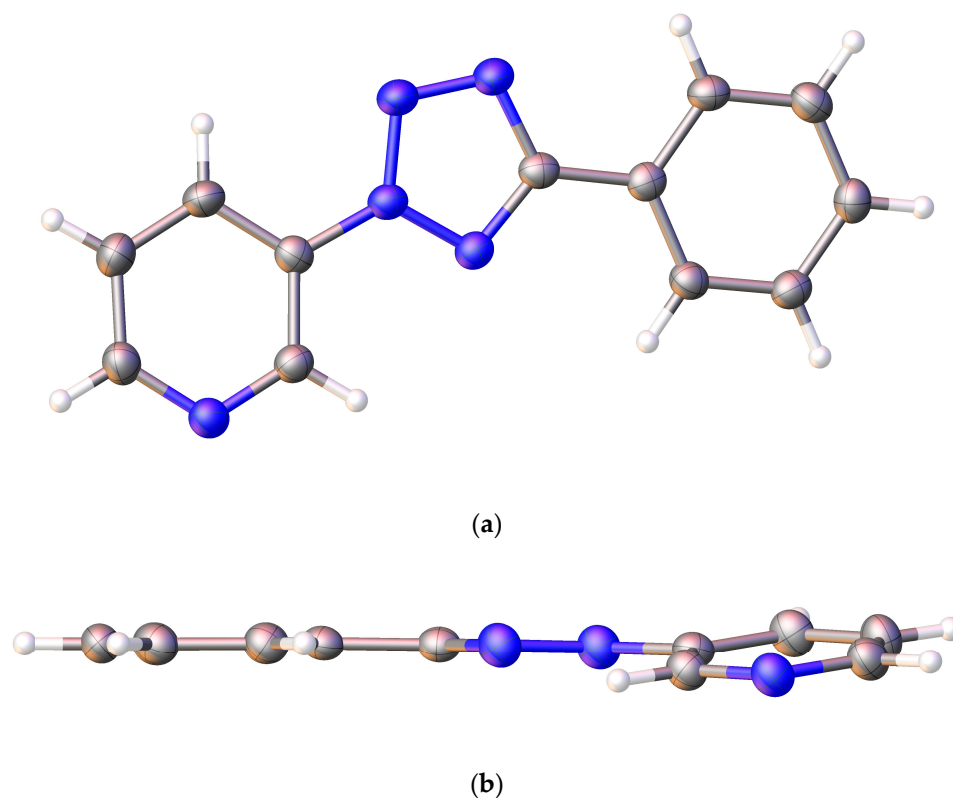


**Figure 3.** Structure of compound 1 obtained from X-ray diffraction analysis: (a) front view; (b) side view.

The crystal data for compound 1 are presented in Table 1.

**Table 1.** Crystal data and structure refinement parameters for 3-(5-phenyl-2H-tetrazol-2-yl)pyridine 1.

Crystal Data	Structure Refinement Parameters
CCDC number	2,237,254
Empirical formula	C <sub>12</sub> H <sub>9</sub> N <sub>5</sub>
Molecular mass	223.24
Temperature, K	100(2)
Crystal system	monoclinic
Space group	I2/a
a, Å	20.8450(9)
b, Å	4.6353(2)
c, Å	22.7163(11)
α, °	90
β, °	107.329(5)
γ, °	90
Volume, Å <sup>3</sup>	2095.29(17)
Z	8
ρ <sub>calc</sub> , g/cm <sup>3</sup>	1.415
μ, mm <sup>-1</sup>	0.744
F(000)	928.0
Crystal size/mm <sup>3</sup>	0.12 × 0.04 × 0.02
Radiation	Cu Kα (λ = 1.54184)
2θ range for data collection/°	8.154 to 138.37
Index ranges	−25 ≤ h ≤ 25, −5 ≤ k ≤ 3, −27 ≤ l ≤ 27
Reflections collected	7480
Independent reflections	1949 [R <sub>int</sub> = 0.0263, R <sub>sigma</sub> = 0.0262]
Data/restraints/parameters	1949/0/154
Goodness-of-fit on F <sup>2</sup>	1.064
Final R indices [I ≥ 2σ(I)]	R <sub>1</sub> = 0.0386, wR <sub>2</sub> = 0.0966
Final R indices [all data]	R <sub>1</sub> = 0.0433, wR <sub>2</sub> = 0.0996
Largest diff. peak/hole/e Å <sup>-3</sup>	0.17/−0.18

The molecular structure of 3-(5-phenyl-2*H*-tetrazol-2-yl)pyridine **1** obtained by X-ray analysis with the numbering of atoms is given in Figure 4.

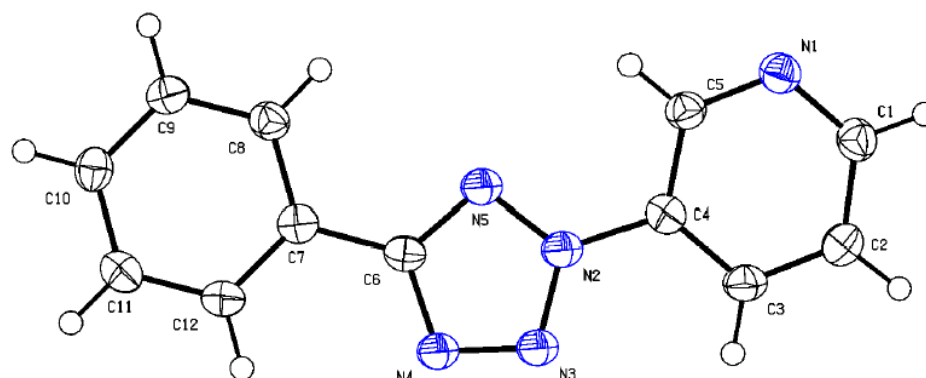


**Figure 4.** Molecular model of 3-(5-phenyl-2*H*-tetrazol-2-yl)pyridine **1** with the numbering of atoms.

Obviously, two different rotamers, which were formed by the rotation of the pyridine heterocycle through the N2-C4 bond, are possible for compound **1** (Figure 5).

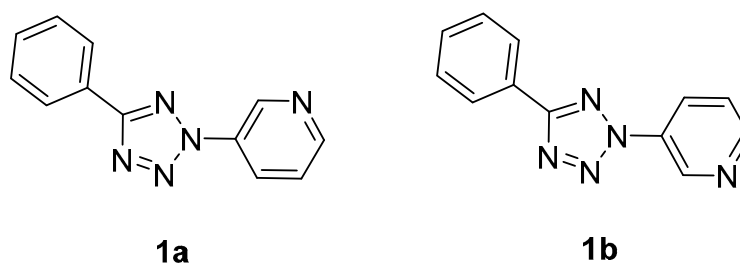


**Figure 5.** Rotamers of 3-(5-phenyl-2*H*-tetrazol-2-yl)pyridine **1a**, **1b**.

Energies (*E*) and dipole moments ( $\mu$ ) of different rotamers of 3-(5-phenyl-2*H*-tetrazol-2-yl)pyridine **1** are shown in Table 2.

**Table 2.** Energies (*E*) and dipole moments ( $\mu$ ) of different rotamers of 3-(5-phenyl-2*H*-tetrazol-2-yl)pyridine **1** calculated by means of DFT B3LYP method in the gas phase and ethanol (IEFPCM model).

Rotamer	Basis Set and Solvation Model				
	6-311+G(d,p), Gas Phase		aug-cc-pVQZ, Gas Phase		6-311+G(d,p), Ethanol
	<i>E</i> , au	$\mu$ , D	<i>E</i> , au	$\mu$ , D	<i>E</i> , au
<b>1a</b>	−736.38507	0.34	−736.71644	0.33	−736.39514
<b>1b</b>	−736.38479	3.83	−736.71618	3.68	−736.39508
$\Delta E^*$ , kcal/mol	0.17		0.16		0.04

\* Energy of rotamer **1a** is equal to 0.

As can be seen in Table 3, according to the X-ray data, this compound has a structure close to planar, and the torsion angle between the phenyl substituent and tetrazole cycle is about 180 degrees, whereas the angle between the planes of the tetrazole and pyridine heterocycles is about 11 degrees.

In the second case, we can assume that the conjugation between the fragments is somewhat weaker because of the somewhat lower aromaticity of the heterocycles compared to that of the benzene cycle. According to the quantum chemical calculation, the absolute planar conjugated structure of the compound is observed. The geometrical parameters given in Table 3 are in good correspondence with the known data for 2,5-disubstituted 2*H*-tetrazoles [24,25]. The values of bond lengths and valence angles determined experimentally in the crystal and calculated theoretically are generally in good agreement with

each other. A slightly better accordance is observed for the case when the influence of the polar solvent is taken into account. At the same time, calculations in the basis set aug-cc-pVQZ do not improve the agreement.

**Table 3.** Selected geometrical parameters of most preferable rotamer 3-(5-phenyl-2H-tetrazol-2-yl)pyridine **1a** obtained by X-ray analysis and calculated by DFT B3LYP method at different basis sets in the gas phase and ethanol (IEFPCM model).

Parameter	X-ray, exp.	DFT B3LYP, Calculated		
		6-311+G(d,p) Gas Phase	6-311+G(d,p) Ethanol	aug-cc-pVQZ Gas Phase
Bond lengths, angstroms				
N1–C1	1.344	1.336	1.338	1.332
C5–N1	1.336	1.333	1.335	1.329
N2–C4	1.424	1.421	1.423	1.417
N2–N3	1.337	1.337	1.333	1.331
N3–N4	1.315	1.299	1.303	1.296
N4–C6	1.363	1.366	1.365	1.362
C6–N5	1.331	1.331	1.331	1.327
N5–N2	1.337	1.332	1.331	1.328
C7–C6	1.461	1.465	1.466	1.462
Bond angles, degrees				
N2–C4–C5	119.5	120.0	119.8	120.1
C3–C4–N2	120.4	120.3	120.4	120.3
N3–N2–C4	122.7	123.0	123.1	120.0
Torsion angles, degrees				
C8–C7–C6–N5	0	0	0	0
N3–N2–C4–C3	11.7	0	0	0

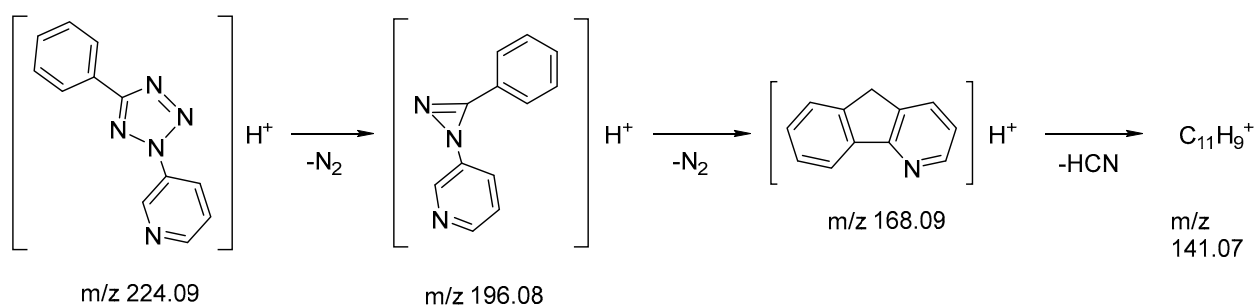
#### 2.4. UV–Vis Spectroscopy

UV–Vis absorption spectrum of 3-(5-phenyl-2H-tetrazol-2-yl)pyridine **1** in ethanol was recorded experimentally (Figure S5, Supplementary Materials) and also calculated by means of TD-SCF approach using DFT and B3LYP functional at 6-311+G(dp) level in ethanol (IEFPCM model). According to the experimental results obtained, the spectrum contains three main bands  $\lambda_{\max}$ , nm ( $\epsilon_{\max}$ , l mol<sup>-1</sup> cm<sup>-1</sup>): 274 (23,600); 236 (26,200), and 202 (about 40,000), and the long-wave band exhibits a clear vibrational structure. The results of quantum-chemical calculations for rotamer **1a** agree satisfactorily with the experimental data. Thus, the absorption bands for **1a** include several singlet electronic transitions, among the major ones are the following,  $\lambda$ , nm (f): 302 (0.46); 260 (0.06); 256 (0.37); 238 (0.1); 223(0.02); 216 (0.21); 210 (0.17); and 195 (0.37).

#### 2.5. Mass-Spectrometry

In order to confirm the structure of the synthesized compound and study the pathways of mass spectrometric fragmentation, high-resolution mass spectra in full scan mode and tandem spectra using electrospray mass spectrometry (ESI–MS) in positive mode were obtained. Due to the presence of N atoms in the structure, the experimental compound can be protonated easily. Despite this, in the spectrum recorded in full scan regime, the signal with  $m/z$  224.09325, which corresponds to  $[M + H]^+$  with error 0.8 ppm, was recorded with relative abundance of only 10% (Table 4, Scheme 4). We can assume that the capillary temperature of 150 °C causes fragmentation of the protonated molecule of the studied compound already in the source. The most intensive signal in full scan spectrum was  $m/z$  196.08716. The best possible molecular formula for this ion was C<sub>12</sub>H<sub>10</sub>N<sub>3</sub><sup>+</sup> (error 1.2 ppm), which could be attributed to the structure  $[M + H - N_2]^+$ . The same pattern was noted by

Fraser and Haque for 2-methyl-5-phenyl-2*H*-tetrazole, which involved loss of nitrogen from the weak molecular ion to give the base peak [26], but further fragmentation was different. In our study, structure  $[M + H - N_2]^+$  remained quite stable due to the conjugated structure. Further fragmentation of this ion with the elimination of the second nitrogen molecule was observed in tandem analysis (CID mode, applied fragmentation energy 35%), the most intense signal with  $m/z$  168.08091 corresponds to the formula  $C_{12}H_{10}N^+$  (error 0.8 ppm). Similar mass-fragmentation was mentioned by Shurukhin and colleagues in the case of the 5-aryl(heteroaryl)tetrazoles elimination of two molecules of  $N_2$  from the molecular ion [27]. In addition, in the tandem spectrum, a signal with  $m/z$  141.0699 of low intensity was noted, corresponding to the  $C_{11}H_9^+$  structure with an error of 0.2 ppm, which could be formed after the detachment of the HCN molecule from the pyridine ring.



**Scheme 4.** Proposed fragmentation pathways for the 3-(5-phenyl-2*H*-tetrazol-2-yl)-pyridine **1**.

**Table 4.** ESI-MS<sup>n</sup> data (relative abundance, %).

MS <sup>n</sup>	Precursor Ions	Fragments Accurate Mass (Intensity, %)	Best Possible Ion Formulae	Error in ppm	Possible Structure
MS <sup>1</sup>	–	224.09325 (10)	$C_{12}H_{10}N_5^+$	0.795	$[M + H]^+$
MS <sup>1</sup>	–	196.08716 (100)	$C_{12}H_{10}N_3^+$	1.204	$[M + H - N_2]^+$
MS <sup>2</sup>	196.08716	168.08091 (100)	$C_{12}H_{10}N^+$	0.798	$[M + H - 2N_2]^+$
MS <sup>2</sup>	196.08716	141.0699 (2)	$C_{11}H_9^+$	0.164	$[M + H - 2N_2 - HCN]^+$

## 2.6. NMR Spectroscopy

<sup>1</sup>H and <sup>13</sup>C-NMR spectroscopy was used to identify 3-(5-phenyl-2*H*-tetrazol-2-yl)-pyridine **1** (Figures S1 and S2). According to the <sup>1</sup>H-NMR spectrum, one can unambiguously identify the signals of protons with  $\delta$  9.37, 8.83, 8.57, and 7.78–7.74 ppm as pyridine ring protons; proton signals with  $\delta$  8.22–8.16 and 7.68–7.57 ppm belong to the phenyl group.

It is known that the chemical shift of the carbon of the 2,5-disubstituted and 1,5-disubstituted tetrazole ring differs by about 10 ppm. For example, for 1-methyl-5-phenyltetrazole  $\delta$  = 154.2 ppm, and for 2-methyl-5-phenyltetrazole  $\delta$  = 164.25 ppm [1]. The obtained data of the chemical shift of the carbon of compound **1** ( $\delta$  = 164.85 ppm) unambiguously show the formation of the N2-isomer, which indicates the selectivity of the reaction. The formation of the N2-isomer is also confirmed by X-ray diffraction analysis.

## 3. Materials and Methods

### 3.1. Synthesis of 3-(5-Phenyl-2*H*-tetrazol-2-yl)-pyridine **1**

The commercial samples of 5-phenyl-1*H*-tetrazole (CAS 18039-42-4, Acros Organics) and pyridin-3-ylboronic acid (CAS 1692-25-7, Boron molecular) were used.

To a solution of 0.297 g (2.03 mmol) of 5-phenyl-1*H*-tetrazole **2** in 12 mL of dry DMSO 0.5 g (4.07 mmol) of pyridin-3-ylboronic acid **3**, 0.05 g (5% mol.) of Cu<sub>2</sub>O and 0.7 g of 4 Å molecular sieves (4 Å MS) were added. Then, oxygen gas was bubbled through the obtained suspension. The reaction mixture was stirred for 15 h at 100 °C using calcium chloride tube to prevent access of air moisture. After cooling to room temperature, a suspension was filtered, and the obtained filtrate was diluted with 50 mL of water and extracted with ethyl

acetate (3 × 15 mL). The organic layers were combined and dried over anhydrous Na<sub>2</sub>SO<sub>4</sub>, filtered, and evaporated. The residue was purified by column chromatography on silica gel (petroleum ether/ethyl acetate = 4/1) to afford the corresponding coupled product (1.77 mmol, 0.395 g, 87%) as a colorless crystal, mp: 125–126 °C. <sup>1</sup>H-NMR (400 MHz, DMSO-*d*<sub>6</sub>) δ, ppm: 9.37 (d, *J* = 2.6 Hz, 1H), 8.83 (dd, *J* = 4.8, 1.5 Hz, 1H), 8.57 (ddd, *J* = 8.3, 2.7, 1.5 Hz, 1H), 8.22–8.16 (m, 2H), 7.78–7.74 (dd, *J* = 8.3, 4.8 Hz, 1H), and 7.68–7.57 (m, 3H). <sup>13</sup>C-NMR spectrum (101 MHz, DMSO-*d*<sub>6</sub>) δ, ppm: 164.85, 151.09, 141.09, 131.17, 129.43, 128.00, 126.75, and 124.87. ESI-MS: Calcd. for [C<sub>12</sub>H<sub>9</sub>N<sub>5</sub> + H]<sup>+</sup>: 224.09361, Found: 224.09325. FT-IR (KBr, cm<sup>-1</sup>): 3442, 3074 (C–H, ν), 2924 (C–H, ν), 2853 (C–H, ν), 1583 (C–C, ν), 1530 (C–C, ν), 1484 (C–C, ν), 1450 (C–C, ν), 1286, 1216, 1194, 1021, 1009, 991, 814, 791, 733, 693, 681, and 615.

### 3.2. Materials and Equipment

#### 3.2.1. Mass-Spectrometry

The target compound was identified by high-performance liquid chromatography–high-resolution mass spectrometry (HPLC–MS–HR) using a Prominence LC–20 HPLC system (Shimadzu, Duisburg, Germany) in combination with an LTQ Orbitrap XL mass spectrometer (Thermo Fisher Scientific, San Jose, CA, USA). A Luna Omega C18 reverse phase column (100 × 2.1 mm, 3 μm, Phenomenex, Torrance, CA, USA) was used in the gradient elution mode at a flow rate of 0.3 mL/min with a mixture of water and acetonitrile. Mass spectrometric analysis was performed under electrospray ionization conditions in the positive ion detection mode. Ion mass scanning range was *m/z* 70–250. Capillary temperature was 150 °C. The target compound was identified based on accurate ion mass measurements with a resolution of 30,000 and accuracy within 5 ppm. Fragment spectra were obtained in a linear ion trap, the collision energy was 35% in the CID mode (Collision Initiated Dissociation).

#### 3.2.2. Differential Scanning Calorimetry (DSC)

Differential scanning calorimetry (DSC) was performed using a Shimadzu DSC-60 Plus differential scanning calorimeter (Kyoto, Japan). The analysis was carried out in N<sub>2</sub> atmosphere (flow rate 100 mL/min) with samples of approximately 2.8 mg at a scanning speed of 3, 10, 20, and 30 °C/min in the temperature range from 273 to 573 K. Data processing was carried out using the ShimadzuCorporation@ta60 Version 2.21.

#### 3.2.3. X-ray Diffraction Analysis

A suitable crystal was studied using Rigaku «XtaLAB Synergy-S» diffractometer (monochromated Cu Kα radiation, λ = 1.54184 Å). The temperature was kept at 100 K throughout the experiment. Empirical absorption correction was applied in CrysAlisPro (Agilent Technologies, 2014) program complex using spherical harmonics, implemented in SCALE3 ABSPACK scaling algorithm. The structures were solved by SHELXT [28] program, using least squares minimization in anisotropic (for non-hydrogen atoms) approximation and refined with the SHELXL package [29] incorporated in the Olex2 program package [30]. The hydrogen atoms were introduced to the geometrically calculated positions and refined by attaching themselves to the corresponding parent atoms.

Supplementary crystallographic data for this paper have been deposited at Cambridge Crystallographic Data Centre (CCDC 2237254) and can be obtained free of charge via [www.ccdc.cam.ac.uk/data\\_request/cif](http://www.ccdc.cam.ac.uk/data_request/cif), accessed on 8 February 2023.

#### 3.2.4. NMR Spectroscopy

The solution <sup>1</sup>H, <sup>13</sup>C-NMR spectra were recorded on a Bruker Avance III 400 MHz spectrometer in DMSO-*d*<sub>6</sub>.

### 3.2.5. IR Spectroscopy

Spectra were registered using Infrared Fourier spectrometer Shimadzu IRAffinity-1 in KBr and attenuated total reflectance (ATR) accessory, model Quest Single Reflection (SPECAC).

### 3.2.6. UV–Vis Spectroscopy

UV-Spectra were registered using UV–Vis spectrometer Shimadzu 2401 in ethanol.

### 3.2.7. Quantum Chemistry Calculation

All calculations were performed using density functional theory (DFT) approach and B3LYP as functional using the Gaussian16 software package [31]. Molecules visualization was carried out in GaussView 6.0 [32]. Geometry optimization, and energy and frequency calculations were calculated using 6-311+G(d,p) and aug-cc-pVQZ as basis sets and IEFPCM model (ethanol,  $\epsilon = 24.852$ ) model to take into account indirect impact of a solvent. All stationary points were proved to be minima by frequency calculations at the same level. Zero-point and thermal corrections ( $T = 298.15$  K) to total energy have been made in the case of B3LYP/6-311+G(d,p).

## 4. Conclusions

As a result of Chan–Evans–Lam cross-coupling of 5-phenyl-1*H*-tetrazole and pyridine-3-ylboronic acid, 3-(5-phenyl-2*H*-tetrazol-2-yl)pyridine **1** was obtained in 87% yield. The structure and identity of compound **1** were confirmed by precision instrumental methods, including X-Ray analysis,  $^1\text{H}$ ,  $^{13}\text{C}$ -NMR spectroscopy, high-resolution mass spectrometry, IR spectroscopy, UV–Vis spectroscopy, and differential scanning calorimetry. X-ray diffraction analysis and UV–Vis spectroscopy data are compared with the results of ab initio quantum-chemical calculations. It is assumed that in the gas phase and ethanol solution, compound **1**, in contrast to the crystal, may exist as two rotamers **1a**, **1b**. Rotamer **1a**, which has lower energy, predominates. In the near future, we plan to investigate the in vitro and in vivo multitarget activity of 3-(5-phenyl-2*H*-tetrazol-2-yl)pyridine **1** in accordance with computer prediction data.

**Supplementary Materials:** The following supporting information can be downloaded online, Figure S1:  $^1\text{H}$ -NMR spectrum of 3-(5-phenyl-2*H*-tetrazol-2-yl)-pyridine in  $\text{DMSO-}d_6$ ; Figure S2:  $^{13}\text{C}$ -NMR spectrum of 3-(5-phenyl-2*H*-tetrazol-2-yl)-pyridine in  $\text{DMSO-}d_6$ ; Figure S3: IR spectrum of 3-(5-phenyl-2*H*-tetrazol-2-yl)-pyridine (in KBr); Figure S4: DSC thermogram of 3-(5-phenyl-2*H*-tetrazol-2-yl)pyridine; Figure S5: UV–Vis absorption spectrum of 3-(5-phenyl-2*H*-tetrazol-2-yl)pyridine.

**Author Contributions:** Conceptualization, V.A.O.; methodology, O.M.N., K.A.E. and V.A.O.; formal analysis, E.V.S., A.M.P., O.M.N., E.N.C., Y.N.P., A.V.K. and R.E.T.; investigation, I.S.E., K.A.E., E.N.C., I.S.C., O.M.N., A.V.K., R.E.T., M.A.S., N.T.S. and V.A.O.; resources, E.N.C., K.A.E., E.V.S. and A.M.P.; data curation, A.V.K., M.A.S., I.S.E., R.E.T. and V.A.O.; writing—original draft preparation, E.V.S., V.A.O., E.N.C., A.V.K., M.A.S., N.T.S., I.S.E. and Y.N.P.; writing—review and editing, M.A.S.; project administration, V.A.O. All authors have read and agreed to the published version of the manuscript.

**Funding:** This research was funded by the Russian Foundation for Basic Research and the Committee on Science of the Republic of Armenia within the framework of the scientific project No. 20-53-05010 Arm\_a/20RF-138 and by the grant program for young scientists FASIE (2022–2023) No. 17837GU/2022.

**Institutional Review Board Statement:** Not applicable.

**Informed Consent Statement:** Not applicable.

**Data Availability Statement:** Not applicable.

**Acknowledgments:** The authors are grateful to the Engineering Center of the St. Petersburg State Technological Institute and the Research Park of St. Petersburg State University for their technical support.

**Conflicts of Interest:** The authors declare no conflict of interest.

**Sample Availability:** Samples of the compounds are not available from the authors.

## References

- Ostrovskii, V.A.; Popova, E.A.; Trifonov, R.E. Tetrazoles. In *Comprehensive Heterocyclic Chemistry*, 4th ed.; Black, D., Cossy, J., Stevens, C., Eds.; Elsevier: Oxford, UK, 2022; Volume 6, pp. 182–232. [[CrossRef](#)]
- Popova, E.A.; Trifonov, R.E.; Ostrovskii, V.A. Tetrazoles for Biomedicine. *Russ. Chem. Rev.* **2019**, *88*, 644–676. [[CrossRef](#)]
- Herr, R.J. 5-Substituted-1H-tetrazoles as Carboxylic Acid Isosteres: Medicinal Chemistry and Synthetic Methods. *Bioorg. Med. Chem.* **2002**, *10*, 3379–3393. [[CrossRef](#)] [[PubMed](#)]
- Trifonov, R.E.; Ostrovskii, V.A. Protolytic Equilibria in Tetrazoles. *Russ. J. Org. Chem.* **2006**, *42*, 1585–1605. [[CrossRef](#)]
- Filimonov, D.A.; Lagunin, A.A.; Glorizova, T.A.; Rudik, A.V.; Druzhilovskii, D.S.; Pogodin, P.V.; Poroikov, V.V. Prediction of the Biological Activity Spectra of Organic Compounds Using the Pass Online Web Resource. *Chem. Heterocycl. Compd.* **2014**, *50*, 444–457. [[CrossRef](#)]
- Ostrovskii, V.A.; Danagulyan, G.G.; Nesterova, O.M.; Pavlyukova, Y.N.; Tolstyakov, V.V.; Zarubina, O.S.; Slepukhin, P.A.; Esaulkova, Y.L.; Muryleva, A.A.; Zarubaev, V.V.; et al. Synthesis and antiviral activity of nonannulated tetrazolylpyrimidines. *Chem. Heterocycl. Compd.* **2021**, *57*, 448–454. [[CrossRef](#)]
- Lippmann, E.; Könnecke, A. 2-Aryltetrazoles—Synthese und Eigenschaften. *Z. Chem.* **1976**, *16*, 90–100. [[CrossRef](#)]
- Shawali, A.S.; Fahmi, A.A.; Eweiss, N.F. Azo Coupling of Benzenesulfonylhydrazones of Heterocyclic Aldehydes. *J. Heterocycl. Chem.* **1979**, *16*, 123–128. [[CrossRef](#)]
- Beletskaya, I.P.; Davydov, D.V.; Gorovoy, M.S. Palladium- and copper-catalyzed selective arylation of 5-aryltetrazoles by diaryliodonium salts. *Tetrahedron Lett.* **2002**, *43*, 6221–6223. [[CrossRef](#)]
- Chan, D.M.T.; Monaco, K.L.; Wang, R.-P.; Winters, M.P. New N- and O-Arylations with Phenylboronic Acids and Cupric Acetate. *Tetrahedron Lett.* **1998**, *39*, 2933–2936. [[CrossRef](#)]
- Evans, D.A.; Katz, J.L.; West, T.R. Synthesis of Diaryl Ethers through the Copper-Promoted Arylation of Phenols with Arylboronic Acids. An Expedient Synthesis of Thyroxine. *Tetrahedron Lett.* **1998**, *39*, 2937–2940. [[CrossRef](#)]
- Lam, P.Y.; Clark, C.G.; Saubern, S.; Adams, J.; Winters, M.P.; Chan, D.M.; Combs, A. New Aryl/Heteroaryl C-N Bond Cross-coupling Reactions via Arylboronic Acid/Cupric Acetate Arylation. *Tetrahedron Lett.* **1998**, *39*, 2941–2944. [[CrossRef](#)]
- Abedinifar, F.; Mahdavi, M.; Rezaei, E.B.; Asadi, M.; Larijani, B. Recent Developments in Arylation of N-Nucleophiles via Chan-Lam Reaction: Updates from 2012 Onwards. *Curr. Org. Synth.* **2022**, *19*, 16–30. [[CrossRef](#)] [[PubMed](#)]
- Mallia, C.J.; Burton, P.M.; Smith, A.M.R.; Walter, G.C.; Baxendale, I.R. Baxendale Ian R. Catalytic Chan-Lam coupling using a ‘tube-in-tube’ reactor to deliver molecular oxygen as an oxidant. *Beilstein J. Org. Chem.* **2016**, *12*, 1598–1607. [[CrossRef](#)]
- Chen, J.; Li, J.; Dong, Z. A Review on the Latest Progress of Chan-Lam Coupling Reaction. *Adv. Synth. Catal.* **2020**, *362*, 3311–3331. [[CrossRef](#)]
- Siva Reddy, A.; Ranjith Reddy, K.; Nageswar Rao, D.; Jaladanki, C.K.; Bharatam, P.V.; Lam, P.Y.S.; Das, P. Copper(II)-catalyzed Chan-Lam cross-coupling: Chemoselective N-arylation of aminophenols. *Org. Biomol. Chem.* **2017**, *15*, 801–806. [[CrossRef](#)] [[PubMed](#)]
- Vantourout, J.C.; Miras, H.N.; Isidro-Llobet, A.; Sproules, S.; Watson, A.J.B. Spectroscopic Studies of the Chan-Lam Amination: A Mechanism-Inspired Solution to Boronic Ester Reactivity. *J. Am. Chem. Soc.* **2017**, *139*, 4769–4779. [[CrossRef](#)] [[PubMed](#)]
- Onaka, T.; Umemoto, H.; Miki, Y.; Nakamura, A.; Maegawa, T. [Cu(OH)(TMEDA)]<sub>2</sub>Cl<sub>2</sub>-Catalyzed Regioselective 2-Arylation of 5-Substituted Tetrazoles with Boronic Acids under Mild Conditions. *J. Org. Chem.* **2014**, *79*, 6703–6707. [[CrossRef](#)]
- Motornov, V.; Latyshev, G.V.; Kotovshchikov, Y.N.; Lukashev, N.V.; Beletskaya, I.P. Copper(I)-Catalyzed Regioselective Chan-Lam N<sup>2</sup>-Vinylolation of 1,2,3-Triazoles and Tetrazoles. *Adv. Synth. Catal.* **2019**, *361*, 3306–3311. [[CrossRef](#)]
- Liu, C.-Y.; Li, Y.; Ding, J.-Y.; Dong, D.-W.; Han, F.-S. The Development of Copper-Catalyzed Aerobic Oxidative Coupling of NH-Tetrazoles with Boronic Acids and an Insight into the Reaction Mechanism. *Chem. Eur. J.* **2014**, *20*, 2373–2381. [[CrossRef](#)]
- Wentrup, C.; Kvaskoff, D. 1,5-(1,7)-Biradicals and Nitrenes Formed by Ring Opening of Hetaryl nitrenes. *Aust. J. Chem.* **2013**, *66*, 286–296. [[CrossRef](#)]
- Jamieson, C.; Livingstone, K. The Nitrile Imine 1,3-Dipole. In *Properties, Reactivity and Applications*; Springer Nature Switzerland AG: Cham, Switzerland, 2020. [[CrossRef](#)]
- Bégué, D.; Dargelos, A.; Wentrup, C. Aryl Nitrile Imines and Diazo Compounds. Formation of Indazole, Pyridine N-Imine, and 2-Pyridyldiazomethane from Tetrazoles. *J. Org. Chem.* **2020**, *85*, 7952–7958. [[CrossRef](#)] [[PubMed](#)]
- Ostrovskii, V.A.; Koldobskii, G.I.; Trifonov, R.E. Tetrazoles. In *Comprehensive Heterocyclic Chemistry*, 3rd ed.; Katritzky, A.R., Ramsden, C.A., Scriven, E.F.V., Taylor, R.J.K., Eds.; Elsevier: Oxford, UK, 2008; ISBN-13: 978-0-0804-4991-3.
- Trifonov, R.E.; Alkorta, I.; Ostrovskii, V.A.; Elguero, J. A theoretical study of the tautomerism and ionization of 5-substituted NH-tetrazoles. *J. Mol. Struct. THEOCHEM* **2004**, *668*, 123–132. [[CrossRef](#)]
- Fraser, R.R.; Haque, K.E. Nuclear magnetic resonance and mass spectral properties of 5-aryltetrazoles. *Can. J. Chem.* **1968**, *46*, 2855–2859. [[CrossRef](#)]
- Shurukhin, Y.V.; Klyuev, N.A.; Grandberg, I.I. Similarities between thermolysis and mass spectrometric fragmentation of tetrazoles (Review). *Chem. Heterocycl. Compd.* **1985**, *21*, 605–620. [[CrossRef](#)]
- Sheldrick, G.M. SHELXT—Integrated space-group and crystal-structure determination. *Acta Cryst.* **2015**, *A71*, 3–8. [[CrossRef](#)] [[PubMed](#)]

29. Sheldrick, G.M. Crystal structure refinement with SHELXL. *Acta Cryst.* **2015**, *C71*, 3–8. [[CrossRef](#)]
30. Dolomanov, O.V.; Bourhis, L.J.; Gildea, R.J.; Howard, J.A.K.; Puschmann, H. OLEX2: A complete structure solution, refinement and analysis program. *J. Appl. Cryst.* **2009**, *42*, 339–341. [[CrossRef](#)]
31. Frisch, M.J.; Trucks, G.W.; Schlegel, H.B.; Scuseria, G.E.; Robb, M.A.; Cheeseman, J.R.; Scalmani, G.; Barone, V.; Petersson, G.A.; Nakatsuji, H.; et al. *Gaussian 16*; revision C.01; Gaussian, Inc.: Wallingford, CT, USA, 2019.
32. Dennington, R.D.; Keith, T.A.; Millam, J.M. *GaussView*, version 6; Semichem Inc.: Shawnee Mission, KS, USA, 2016.

**Disclaimer/Publisher's Note:** The statements, opinions and data contained in all publications are solely those of the individual author(s) and contributor(s) and not of MDPI and/or the editor(s). MDPI and/or the editor(s) disclaim responsibility for any injury to people or property resulting from any ideas, methods, instructions or products referred to in the content.